Hydrogeological and hydrogeochemical characterization of the unconfined aquifer in the fluvio-eolian plain of Cordoba (Argentina)

F. Becher Quinodoz, L. Maldonado, M. Blarasin, V. Lutri, A. Cabrera, M. J. Giuliano Albo and E. Matteoda

ABSTRACT

The studied area, a vast plain located in the South of Córdoba (Argentina), presents a relief resulting from the juxtaposition of an eolian and a fluvial system. The objective of this work was to characterize the unconfined aquifer from a dynamic and a geochemical point of view, establishing relationships with lithological and geomorphological features and validating with statistical multivariate analysis (Q mode) of the geochemical data. The unconfined aquifer presents variable hydraulic gradients and groundwater velocity, both conditioned by the local relief and lithology. The aquifer showed a varied spatial geochemical pattern with fresh to salty water (0.4–10.0 g/L) and sodium bicarbonate to sodium chloride geochemical types, in some places of mixed anionic type. The statistical analysis showed two groups: Group 1 links salty-brackish groundwater of sulfate and chloride type with longitudinal dunes and lowlands with locally outcropping water. It represents evolved groundwater coming from intermediate and regional flows. Group 2 links fresh groundwater of bicarbonate type with active dunes and paleochannels. In these sites, where coarser sediments prevail, local groundwater flow cells develop as a result of recent recharge, leading to greater groundwater velocity and decreasing the transference of ions to solution. These results allow us to identify the most promising areas for freshwater abstraction.

Key words | geomorphology, groundwater, lithology, quality, statistical analysis

F. Becher Quinodoz (corresponding author)
L. Maldonado
V. Lutri
CONICET-UNRC,
Ruta 36 km 602, Rio Cuarto, Córdoba,
Argentina
E-mail: *fbecher@exa.unrc.edu.ar*

M. Blarasin
A. Cabrera
M. J. Giuliano Albo
E. Matteoda
Department of Geology,
Universidad Nacional de Rio Cuarto (UNRC),
Ruta 36 km 602, Rio Cuarto, Córdoba,
Argentina

INTRODUCTION

The unconfined aquifer in the Pampean Plain of the South of Córdoba province in Argentina suffers from typical problems experienced in other areas of the world including high salinity, arsenic and fluorides.

To understand the aquifer behaviour, the study of geomorphology is very useful, linking the relief forms and the lithologies with the groundwater dynamics and quality (Del Pilar Álvarez *et al.* 2010; Chakraborty *et al.* 2011; Álvarez *et al.* 2014; Rajaveni *et al.* 2017). Del Pilar Álvarez *et al.* (2010), Ramaiah *et al.* (2012) and Sedhuraman *et al.* (2014) recognize the importance of geomorphology as a controlling factor of groundwater and delineate different potential zones of groundwater based on different geomorphological units using classical hydrogeological studies. This type of research has allowed the finding of groundwater recharge sectors not affected by pollution processes (Carol *et al.* 2010, 2015; Blarasin *et al.* 2013; Rani *et al.* 2015).

In the case of the Pampean Plain of the South of Córdoba province (Argentina), the most used water resource for all activities is the groundwater contained in the unconfined aquifer. From a geochemical point of view the salinity of this aquifer evolves in the flow direction from fresh waters (calcium and sodium bicarbonate types) in the recharge areas (mainly the piedemont of the occidental Pampean Mountains) to salty waters (sodium chloride type) in distal flat plain or depressed environments (Blarasin *et al.* 2014).

doi: 10.2166/nh.2018.043

The water aptitude for human consumption, livestock and irrigation uses is excellent in the main fluvial strips and decreases noticeably in the flow direction. The less suitable zones for groundwater extraction are those located in the periphery of the province, where sandy and loessical eolian plains domain. Arsenic, fluorine and other trace elements also increase in groundwater contained in eolian aquifers. However, it has been recently proved that in these regions there are local geomorphological-lithological conditions that allow the finding of suitable waters (Blarasin *et al.* 2014).

Taking into account the mentioned problems, a large region (7,000 km^2) in the south of Córdoba was selected for the present research (Figure 1). It is limited by the 33° 50′ and 34° 31′ parallel coordinates (south latitude) and 64° 00′ and 65° 00′ meridians (west longitude).

The goal is to carry out the hydrodynamic and hydrogeochemical characterization of the unconfined aquifer in the fluvio-eolian plain of southern Córdoba, establishing relationships with the main geomorphological-lithological features. Statistical multivariate analysis (Q mode) of the hydrogeochemical data is a significant element of this characterization.

METHODS

The research was carried out at a scale 1:150,000, based on the analysis and compilation of satellite images (Google Earth, LANDSAT ETM +) and topographic charts from the National Geographic Institute (IGN). The climatic characterization of the area was carried out through the treatment and interpretation of the collected information, especially precipitation, a variable that constitutes the main entry function to the studied hydrological system. The precipitation data from the 'El Colorado-El Olvido' station covered a series of 111 years (1903–2014).

The main geological and geomorphological features and outcropping lithological profiles were surveyed, both in the dune area and in the fluvial systems (the Rio Quinto River and the Arroyo Ají stream) during earlier surveys (Bécher Quinodóz 2014) and completed for this work. Information about underground lithological profiles (approximately 50 m deep) taken from regional drillings was collected and interpreted. The forms of the relief were observed and characterized, the active processes were recorded and the geomorphological map of the area was elaborated. The sediment samples from outcrops and boreholes were subjected to textural analysis (ASTM sieves, Udden–Wendworth scale), obtaining the histograms with percentages of the different granulometric fractions. To complement the underground geological reconstruction, geoelectric prospecting was carried out using vertical electric soundings (VES) according to the Schlumberger arrangement (Geometer MPX-400, Ponti Electronics, Mendoza, Argentina). The obtained results were compared with drilling data.

The hydrogeological study was based on a census of 90 wells that extract water from the unconfined aquifer

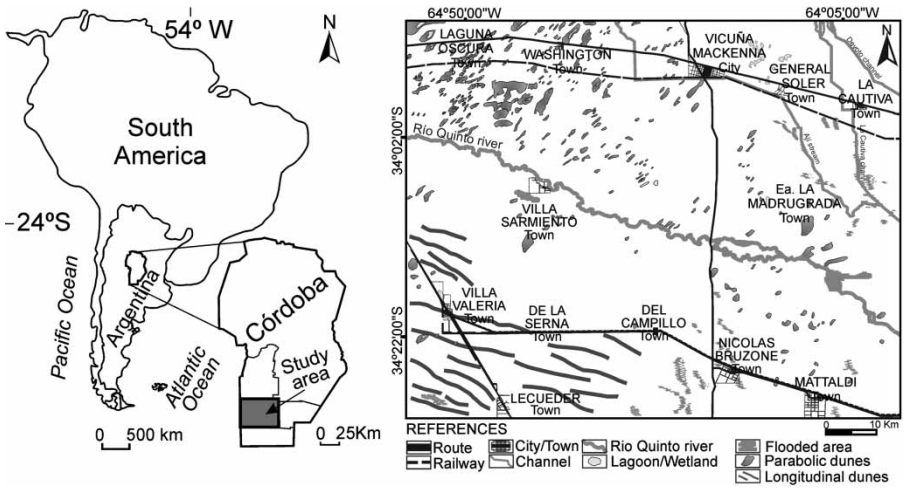

Figure 1 | Study area.

at a maximum depth of 50 m. Information related to lithology and wells (screen length, diameter and depth, flow rates, water level drawdown and so on) was collected. In addition, the water table depths were measured and maps of spatial variation of hydraulic potentials and the water table depth were prepared and interpreted. With both maps and the topographic/geomorphological base, the relationships between the relief and the groundwater were analyzed. In addition, aquifer recharge information was available from a well equipped with a water level data logger, located in the dune field that surrounds the Laguna Oscura lagoon (Bécher Quinodóz *et al.* 2016).

For the hydrochemical study, temperature (T), electrical conductivity (EC), total dissolved solids (TDS) and pH were measured *in situ* with a Hanna multiparametric probe. The physico-chemical analysis was carried out in the Geochemistry Laboratory of the Department of Geology of the National University of Río Cuarto (UNRC). Concentrations of the following ions and compounds were measured: carbonates (CO_3^{2-}) and bicarbonates (HCO_3^-), sulfates (SO_4^{2-}), chlorides (Cl^-), calcium (Ca^{2+}) and magnesium (Mg^{2+}), sodium (Na^+) and potassium (K^+). In all cases, the error of the chemical analysis was <10%. The samples were classified taking into account the ionic composition according to Custodio (1993). Different maps were made to evaluate spatial distribution of water features: salinity (mg/L), the known property that depends directly from EC, HCO_3^-/Cl^- ratio and geochemical types using Stiff diagrams.

As part of the hydrogeochemical characterization, a multivariate statistical analysis was also performed because of the many parameters (nine in total) involved. Multivariate analysis allows the classification and grouping of water samples. A hierarchical clustering technique was employed in the multivariate analysis. This clustering technique is the one that is most widely applied in Earth sciences (Davis 1986), and is often used in the classification of hydrogeochemical data (Güler *et al.* 2002; Cloutier *et al.* 2008). SPSS software V.21 was used to apply the hierarchical cluster method in Q mode.

RESULTS AND DISCUSSION

Climatic characteristics

The regional climate is sub-humid-dry of the mesothermal type, with a mean annual precipitation (MAP) of 750 mm (Figure 2(a)), concentrated mainly in spring–summer. The series 1903–2014 of annual precipitations (P) exhibits a minimum of 119 mm and a maximum of 1,331 mm. The soil water balance, made with a monthly time step, shows that between 58.5% and 100% of P is returned to the atmosphere as actual evapotranspiration. Water deficits occur mainly in the autumn–winter months. The monthly water

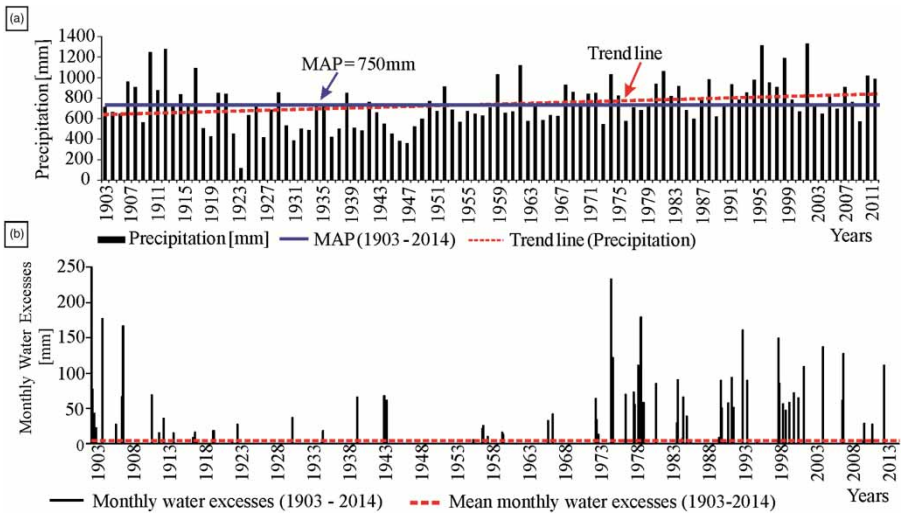

Figure 2 | (a) Annual precipitations; (b) water excesses from soil water balance.

excesses, which can contribute to the surface runoff and/or to the recharge of the unconfined aquifer, were variable between 0 and 204 mm and were located mainly in spring–summer, highly conditioned by the precipitations behavior. The trend of water excesses is growing, mainly from 1972 (Figure 2(b)), explaining the higher river flows and major aquifer recharge in the last four decades (Blarasin *et al.* 2014).

Geological–geomorphological characterization

The study area is located within the Pampean Plain geological province, to the east and southeast of the Pampean Mountains of Córdoba and San Luis. In the latter, the Rio Quinto River, which crosses the study area, develops its upper basin. The study area presents a flat to a gently undulating relief. There is a structural control associated with the typical regional tectonic relief of descending blocks, a geological setting related to the Andean Orogeny. An important regional system of geological structures with NNW–SSE direction is represented in the area by the lineament that controls the Rio Quinto River course (Criado *et al.* 1981; Kostadinoff & Gregori 2004). In addition, the San Basilio and Tigre Muerto regional faults, with NS direction, must be highlighted because of their influence on relief (Degiovanni *et al.* 2005).

The bedrock is neither outcropping in the area nor was it intercepted by the surveyed wells. Gravimetric studies conducted in the Villa Valeria area by Kostadinoff & Gregori (2004) indicate a thick layer of sediments (2,500 m) above the bedrock. The hydrogeological information is available up to approximately 400 m depth. The lower part of this general sequence (between 400 and 100 m) is composed of sediments of the Upper Paleogene–Quaternary. They are continental sediments of eolian origin interlayered with very thin strata of fluvial origin, corresponding to low and high energy fluvial facies (fine, medium and coarse sands with scattered gravels). At a depth of 90–15 m the sediments correspond to typical eolian/alluvial/lagoons deposition sequences (Lower Quaternary). The outcropping recognized materials (the upper 15 m) correspond mostly to eolian deposits pertaining to the Laguna Oscura Formation (Upper Holocene, Cantú (1992)). There are also historical deposits (last centuries) of eolian and alluvial origin. In general, they represent cycles of aggradation controlled by neotectonic events and fundamentally by climatic oscillations (Degiovanni *et al.* 2005; Carignano *et al.* 2014).

From the geomorphological point of view, the area presents only aggradation reliefs of the Upper Pleistocene–Holocene period, resulting from the interaction and interdigitation of the eolian system ('Pampean Sand Sea') with the river system of the Rio Quinto River, which developed alluvial paleofans with apices in different positions. The study area constitutes a composite landscape where three major geomorphological environments were recognized, namely I: Eolian Plain, II: Eolian–Fluvial Plain and III: Fluvial Plain (Figure 3, Table 1).

Taking into account the textural analysis (Figure 4(a)), it is observed that in all the geomorphological units there is a dominance of psamo–pelitic sediments with variable degrees of carbonate cementation. In the fluvial environment, sands with scattered gravels dominate; in the fluvio–eolian environment coarse and very coarse sands are prevalent; while in the eolian environment the fine sand and silty sand fractions dominate. In the low land areas, an increase in the silt–clay percentage was observed. The mineralogical studies previously carried out allowed the identification of the dominance of volcanic glass and minerals such as quartz, plagioclase, potassium feldspar, biotite, amphiboles and pyroxenes, in all the geomorphological units (Bécher Quinodóz 2014).

Hydrogeological and hydrodynamic characterization

The studied unconfined aquifer shows an average thickness of 80 m, whose base is made up of aquitard and aquiclude layers, as is shown in the typical hydrogeological profile of this area (Figure 4(b)). It exhibits moderate homogeneity given the fine sediments' dominance, although local facies changes are recognized which generate anisotropies from the hydraulic point of view (Figure 4(a) and 4(b)). These changes are linked to more cemented materials or to those sectors with coarse and medium sands (some fluvial or eolian areas). The dominant sediments (very fine sands) have hydraulic conductivity (K) values in the order of 1 2 m/d. In the pumping tests carried out in dune areas (Bécher Quinodóz 2014) these values reach up to 5 7 m/d.

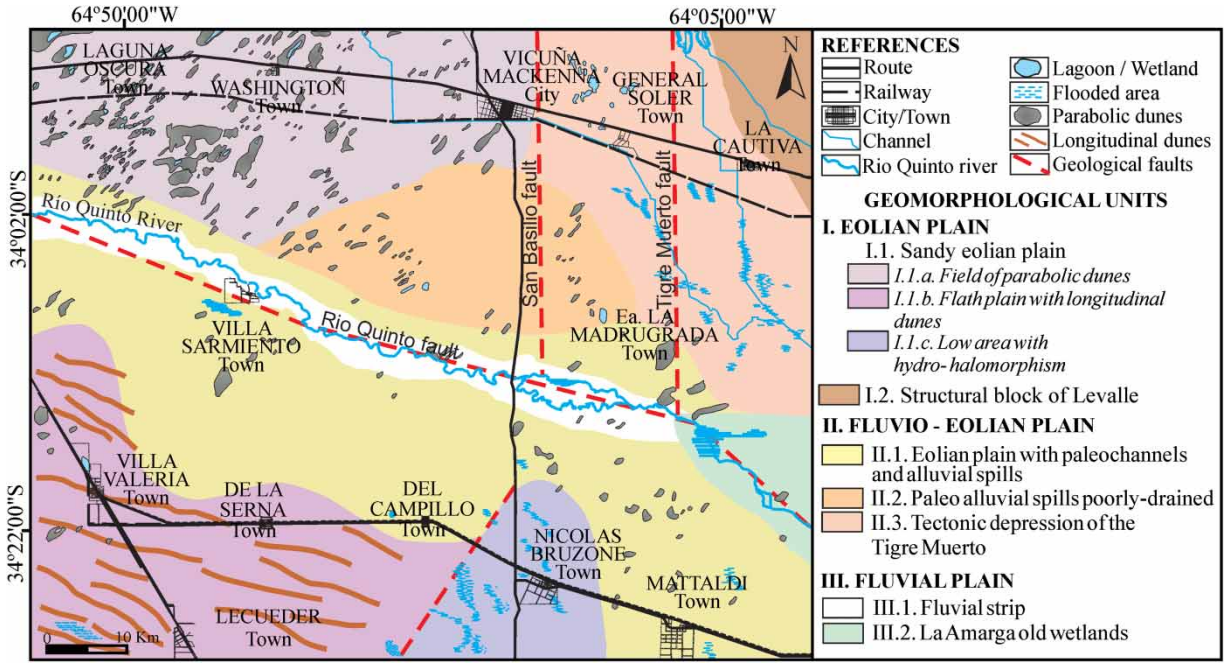

Figure 3 | Geomorphological map.

From the analysis and interpretation of the resistivity curves resulting from VES (vertical electric sounding), the dominance of very fine sand sediments is recognized, interlayered with carbonate cemented levels. These results verify the corresponding lithological records of the regional drillings. The sectors with the best aquifer properties are linked to the fluvial strip of the Rio Quinto River and to the field of the parabolic dunes (Bécher Quinodóz 2014).

The general groundwater flow direction is NW–SE, parallel to the Rio Quinto River course. From the regional point of view the flow lines network (Figure 4(c)) indicates that the area behaves fundamentally as a transit zone of groundwater flow coming from the west. However, the entire eastern sector (east of the Vicuña Mackenna-Del Campillo line) constitutes a depressed area with partial discharge of groundwater, expressed by the presence of small wetlands and lagoons. Local variations in the flow direction are noticed, for example, in the structural block of Levalle, where the flow direction is N–S (Figure 4(c), Table 2). This flow and that coming from the west converge, partially discharging in the low sectors in the La Cautiva–Estancia La Madrugada zone (Figure 4(c)). In the NW dune field, the groundwater flow feeds the NW margin of the lagoons located in the parabolic dunes.

The hydraulic gradients are in the order of 0.09% (lower hydrohalomorphic areas) to 1.5% (dune fields). Using the hydraulic gradients and K, the estimated groundwater velocities are 0.01–0.006 m/d (structural block of Levalle), 0.04–0.07 m/d (central plain) and 0.25–0.5 m/d (dunes and fluvial strip). The depth of the water table is variable, fundamentally because of the topographic characteristics. Thus, the highest values are found in the structural block of Levalle (>10 m) and the lowest (0–2 m) in the depressed areas (Figure 4(c)). The fluctuations of the water table in the last three years have been in the order of 1 m maximum and are fundamentally linked to the aquifer recharge that comes from rainfalls. The water table record obtained in the dune sector (I.I.a in Table 1) shows episodic recharge processes, that is to say, peaks of the water table level immediately after the rains occurred (Bécher Quinodóz *et al.* 2016).

Hydrogeochemical characterization

The results of the physical-chemical analyses are presented in Table 3 and the most important statistical parameters in Table 4. The univariate statistical analysis of the 90 samples (Table 4) allowed us to determine that the total dissolved

Table 1 | Description of geomorphological units

(I) EOLIAN PLAIN:	*(II) FLUVIO-EOLIAN PLAIN:*	*(III) FLUVIAL PLAIN:*
It includes the largest area of the study area. Eolian deposits. Relief gently undulated to flat with slopes of the order of 2%	Relief softly undulated. Slope values less than 0.5% (SE) and locally 3% (in dunes areas). It has present and paleo fluvial and eolian morphologies, occupied mainly by permanent lagoon bodies	Moderately undulating relief, almost flat in the area of wetlands, characterized by a structural control. It is composed of fluvial deposits related to the Rio Quinto River
(I.1.) Sandy eolian plain: part of the large 'Mar de Arena Pampeano' eolian system of the late Pleistocene (Iriondo 1990), with large deflation forms, dune fields and sand deposits I.1.a. Undulated relief with slopes of up to 2%. Old longitudinal dunes (late Pleistocene–Holocene), reworked by NE winds during the Little Ice Age (Tripaldi & Forman 2007) which formed parabolic dunes. Usually permanent lagoons and wetlands occupy the deflation corridors. The local remobilization of sands formed barjanoid chains (NW secondary winds) I.1.b. Gently undulating plain of longitudinal dunes with SE–NW direction (local differences of 2–3 m), slopes lower than 2%. It presents depressions associated with old inter dune deflation corridors I.1.c: Elongated topographic depressions that contain wetlands and lagoons, surrounded by hydro-halomorphic processes linked to the water table fluctuation (I.2.) Structural block of Levalle: great regional hill associated with the 'Tigre Muerto' regional fault. Only a small sector of the southern part is observed in the study area	(II.1.) Eolian plain with paleochannels and paleo-spills. It presents alluvial paleo-fans of the Rio Quinto River, from different climatic stages of the Upper Quaternary. In addition, there are erosive and accumulation eolian geoforms. In discontinuous paleochannels and deflation corridors there are lagoon bodies fed by the water table. Coarser grains appear in the sediments (II.2). Paleo alluvial spills, poorly-drained: located north of the present river channel, is composed of paleochannels and spills of moderate sinuosity characterized by a poor drainage (II.3) Tectonic depression of the Tigre Muerto: It is a low area, with an outcropping or shallow water table level. It corresponds to the sunken block associated with the 'Tigre Muerto' fault, with general slope towards the SSE (in the order of 0.2%) and an asymmetric transversal profile. The area is partially covered by longitudinal dunes from the Middle to Upper Holocene. Current lagoons and wetlands environments are common	(III.1) Fluvial strip: it has an average width of 1 km, reaching a maximum of 3 km near Villa Sarmiento town, where several levels of terraces can be identified. The present course exhibits moderate sinuosity, with high rates of deepening and lateral migration, mainly in recent years. The continuous anthropogenic channeling in La Amarga wetlands reinforced backward erosion processes. Water rapids are common in this sector (III.2) 'La Amarga' old wetland, it is part of the lower basin of the Rio Quinto River. Presents a series of paleochannels and paleo spills related to the epoch in which the area acted as the base level of the river. Currently, this extensive paleo-wetland constitutes a transit area where the course has deepened (6–7 m) and exhibits active vertical incision and processes of lateral erosion. As a result, the spill/discharge area has been moved to more southeastern areas

solid (TDS) has a mean of 3,093 mg/L and a deviation of 2,407.72, which indicates a great variability of this parameter, Figure 5(a).

The results of the hydrogeochemical study show that groundwater with TDS from 0.4 to 1.05 g/L (fresh waters) is linked mainly to the field of parabolic dunes which coincides with a general configuration of preferential recharge sectors from rainwater. The TDS values are in the order of 1.05–1.75 g/L in fluvial sediments of the Rio Quinto River, some sectors of the parabolic dune field and in the structural block of Levalle (Figure 5(a)). In most of the other eolian environments, the TDS are >1.75 g/L (brackish and salt waters). The highest values correspond to low areas (I.1.c; II.2 and III.2 in Table 1) where the water table is close to the surface. In these areas, groundwater discharge occurs with distinctive vegetation, known as 'salinas' or 'playas', in which evapotranspiration at high rates, over a long time, has led to a buildup of salinity. In addition, and given that they are regional depressions which extend beyond the study area, they also receive deeper waters that have traveled long distances; the low flow velocities and longer contact time of the water with the sediments increase the possibility of incorporating solutes into the water (Figure 5(a)).

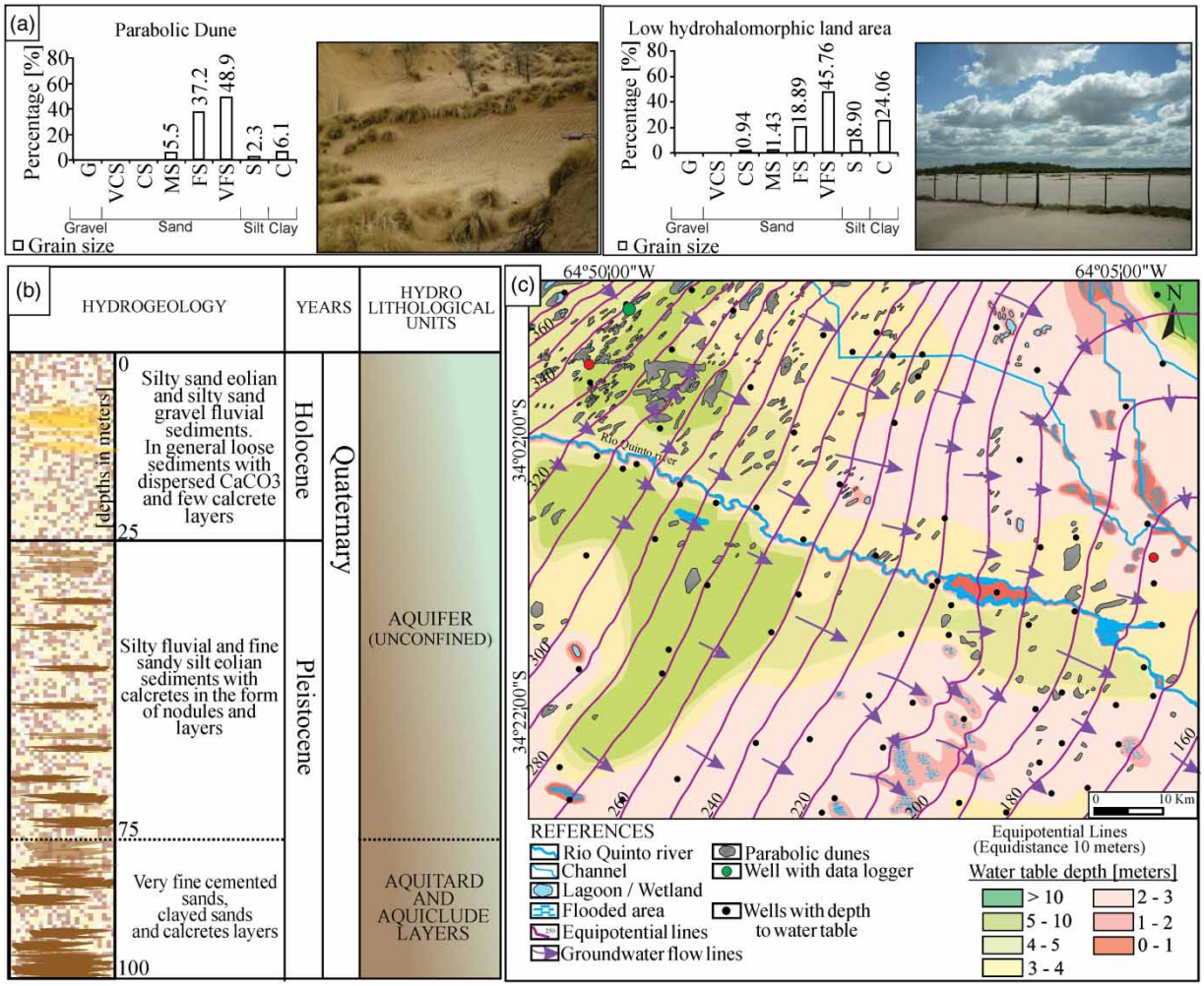

Figure 4 | (a) Textural analysis in two geomorphological environments; (b) hydrogeological general typical profile; (c) equipotential map for the unconfined aquifer and depth of water table.

The geochemical pattern of the groundwater was diverse, showing sodium bicarbonate to sodium chloride types, many of them of mixed anionic type (Figure 5(b)). Thus, groundwater is gradually enriched in sulfates and chlorides as a function of their solubility. In the sector located to the North of the Rio Quinto River, a classical evolution (Tóth 1999) is observed in the flow direction from the west and from the structural block of Levalle towards the center of the depression with groundwater varying from bicarbonate to sulfate types. To the south of the Rio Quinto River the geochemical pattern is greatly conditioned by the geomorphological features (paleochannels, paleospills, dune cover near the river, southern longitudinal dunes) and lithological characteristics. Thus, the freshest waters are conditioned by the influence of preferential recharge on coarser fluvial sediments and active dunes whereas the brackish/salty groundwater is located in the more flat areas with fine sediments.

The ionic ratio $rHCO_3^-/rCl^-$ is useful to identify areas of recharge and discharge of groundwater, as well as to monitor the process of salt concentration in the direction of the groundwater flow. In Figure 6, it is shown that the lowest ratios (<1), revealing waters with a higher Cl^- content, are found in the flat and depressed areas. The long residence times and incomplete flushing of soluble minerals produce groundwater which is generally of the sodium chloride type. The relations >1, with high bicarbonate values, resulting from newly infiltrated waters, are recognized in the NW

Table 2 | Topographic and hydrogeological data

Name	Latitude	Longitude	Well depth (m)	Topographic elevation (m)	Water table depth (m)	Water table level (m)
M2	34°27′01.62″S	64°14′07.44″W	15	185	2.5	182.5
M8	34°21′39.74″S	64°15′26.14″W	15	194	2.5	191.5
M9	34°21′57.15″S	64°12′11.78″W	15	191.9	2.5	189.4
M12	34°22′31.58″S	64°07′21.13″W	20	179.3	2.5	176.8
M14	34°21′48.25″S	64°04′2.01″W	15	174	2.5	171.5
M23	34°25′35.71″S	64°07′12.56″W	20	175	2.5	172.5
M27b	34°25′36.69″S	64°12′15.07″W	20	185	2.5	182.5
M35	34°29′23.69″S	64°13′02.67″W	15	176	2.5	173.5
M37	34°29′01.03″S	64°09′52.10″W	15	180	2.5	177.5
M39	34°28′08.15″S	64°14′30.83″W	15	185	2.5	182.5
M43	34°12′58.33″S	64°23′08.97″W	20	222	3.5	218.5
M44	34°15′00.39″S	64°22′09.06″W	15	222.5	3.5	219
M45	34°18′20.32″S	64°21′21.59″W	20	215.5	2	213.5
M47	34°23′46.30″S	64°21′28.21″W	25	205	2	203
M48	34°26′24.87″S	64°20′26.81″W	20	199.74	2	197.74
M49	34°29′27.71″S	64°21′56.01″W	40	196	2.5	193.5
M51	34°30′59.19″S	64°16′46.96″W	15	183	2	181
M52	34°17′19.15″S	64°14′39.35″W	15	201.5	2	199.5
M53	34°14′08.43″S	64°18′11.59″W	30	212	2.5	209.5
M54	34°17′19.51″S	64°26′37.69″W	15	228.5	2	226.5
M55	34°22′42.06″S	64°25′13.72″W	20	216.5	2.5	214
M56	34°26′02.14″S	64°28′08.92″W	15	216	2.5	213.5
M58	34°31′35.40″S	64°33′47.85″W	20	220	2.5	217.5
M59	34°25′20.69″S	64°34′36.96″W	15	230	2	228
M60a	34°25′53.53″S	64°39′21.98″W	35	241	2	239
M60b	34°25′53.53″S	64°39′21.98″W	35	241	2	239
M61	34°28′39.24″S	64°46′38.77″W	20	256	2.5	253.5
M62	34°30′09.87″S	64°51′17.38″W	20	264	2.5	261.5
M63	34°22′09.50″S	64°29′28.65″W	15	227.64	2	225.64
M64	34°22′32.65″S	64°41′34.92″W	15	253.1	2.5	250.6
M65	34°20′28.18″S	64°55′28.20″W	20	293.25	2.5	290.75
M67	34°19′18.68″S	64°48′23.49″W	15	279.1	8	271.1
M68	34°27′49.63″S	64°57′16.18″W	15	282.5	3.6	278.9
M69	34°13′37.80″S	64°43′23.61″W	15	275	6.32	268.68
M70	34°10′01.01″S	64°48′53.67″W	20	291.6	6.5	285.1
M71a	34°07′11.11″S	64°43′07.02″W	50	280	6.32	273.68
M71b	34°07′11.02″S	64°43′08.58″W	50	280	6.32	273.68
M72	34°05′43.18″S	64°46′30.17″W	15	294	4	290
M74	34°03′24.00″S	64°53′57.82″W	15	309.2	6	303.2
M77	34°11′10.92″S	64°54′28.09″W	15	307	3.5	303.5

(*continued*)

Table 2 | continued

Name	Latitude	Longitude	Well depth (m)	Topographic elevation (m)	Water table depth (m)	Water table level (m)
M79	34°17′14.55″S	64°37′31.74″W	15	255	2.5	252.5
M80a	34°14′25.96″S	64°35′43.23″W	20	252.5	3.5	249
M80b	34°14′08.13″S	64°35′47.31″W	20	252.5	3.5	249
M81	33°55′45.84″S	64°27′18.66″W	15	249	3	246
M82	33°53′54.31″S	64°30′13.25″W	15	265.5	3.5	262
M83	33°54′19.72″S	64°33′45.75″W	20	276.5	3.5	273
M84	33°52′25.14″S	64°41′20.34″W	15	309	3	306
M85	33°50′52.93″S	64°46′25.32″W	15	335	7	328
M86	33°58′11.84″S	64°40′18.85″W	20	291.5	3.5	288
M87	33°59′15.94″S	64°45′52.72″W	15	310	5.3	304.7
M88	33°55′25.34″S	64°46′26.38″W	15	319	2	317
M89	33°57′16.04″S	64°52′56.32″W	15	334.5	2	332.5
M92	34°07′35.72″S	64°39′46.58″W	10	272.5	3	269.5
M93	34°10′18.01″S	64°35′36.18″W	15	254	2	252
M94	34°01′42.31″S	64°36′11.01″W	20	268	3	265
M95	34°01′15.40″S	64°27′26.95″W	20	242.5	2.5	240
M96	34°01′45.36″S	64°27′18.98″W	20	241.5	2.5	239
M97	34°05′39.58″S	64°32′14.47″W	20	253	2.5	250.5
M98	34°11′32.17″S	64°29′01.11″W	15	240	3	237
M99	34°08′19.88″S	64°23′00.64″W	18	223.4	3	220.4
M101	34°10′33.64″S	64°14′19.21″W	15	202.5	3.5	199
M102	34°03′49.22″S	64°16′16.05″W	20	206.5	2.5	204
M103a	33°56′58.51″S	64°25′02.27″W	14	241	3	238
M105a	34°11′19.83″S	64°04′05.74″W	15	178	2.5	175.5
M105b	34°13′17.40″S	64°04′01.46″W	15	178	2.5	175.5
M106	34°09′53.66″S	64°10′53.11″W	15	198.5	3.5	195
M107	33°59′41.66″S	64°06′31.29″W	20	193.5	2.5	191
M108	33°51′13.04″S	64°03′38.92″W	15	214.5	10.5	204
M109	33°53′53.45″S	64°18′36.81″W	15	217.5	2.5	215
M110	33°56′57.11″S	64°14′28.33″W	15	207.5	2.5	205
M111	33°56′11.87″S	64°03′14.74″W	10	195	2.5	192.5
M113	34°16′27.29″S	64°03′22.78″W	15	176.9	2.5	174.4
M114	33°51′45.91″S	64°51′19.74″W	15	348	4	344
M115	33°50′43.19″S	64°56′46.49″W	15	375	2.5	372.5
M116a	33°52′19.11″S	64°51′17.33″W	10	339	6	333
M116b	33°52′19.11″S	64°51′17.33″W	44	339	6	333
M117a	33°53′58.58″S	64°50′44.95″W	15	341	5	336
M117b	33°53′57.55″S	64°50′43.80″W	15	342	5	337
M118	33°57′00.73″S	64°25′00.52″W	15	241.5	3	238.5
M120	34°07′13.55″S	64°42′26.66″W	20	278	5	273

(*continued*)

Table 2 | continued

Name	Latitude	Longitude	Well depth (m)	Topographic elevation (m)	Water table depth (m)	Water table level (m)
M121	34°13′36.98″S	64°23′52.78″W	15	225	4	221
M122	34°15′34.69″S	64°10′53.34″W	20	196	5	191
M123	34°19′43.72″S	64°04′48.45″W	15	178	4	174
M128	34°30′09.55″S	64°56′20.59″W	15	272	2	270
M129	34°30′09.43″S	64°07′31.14″W	15	169	2.5	166.5
M130	33°56′18.04″S	64°02′53.99″W	10	195	2.5	192.5
M131	33°55′38.57″S	64°31′55.40″W	15	264	3	261
M132	33°55′47.98″S	64°24′52.81″W	10	242	3	239
M133	34°08′39.70″S	64°05′16.89″W	10	183.5	2.5	181
M134	34°00′23.59″S	64°12′30.78″W	15	201.5	2.5	199

and SE sectors, associated with the geomorphological units I.1.a. and II.1 (Table 1), sectors where preferential recharge of rainwater occurs.

Statistical multivariate analysis of hydrogeochemical data

As mentioned, the multivariate statistical analysis is a quantitative and independent approach of groundwater classification, allowing the grouping of water samples and the correlations between chemical parameters and samples. In this study, and as is presented in Cloutier *et al.* (2008), the multivariate statistical method was applied to the whole hydrogeochemical dataset that consists of 90 groundwater samples and nine parameters. These parameters include major constituents, HCO_3^-, Cl^-, SO_4^{2-}, Na^+, K^+, Ca^{2+} and Mg^{2+} in addition to EC and pH. For the multivariate statistical analysis, in the total of the 90 samples, values were recorded for all nine parameters, so no filling techniques were carried out.

Thus, the final dataset used for the multivariate statistical analysis is a data matrix of 90 sampling sites (observations) by nine chemical parameters (variables). Table 4 is compiled of the descriptive statistics of the parameters for the 90 groundwater samples. The analysis of the statistical distribution of the parameters shows that the totality is adjusted to the lognormal distribution (Figure 7(a)). Finally, standardization was applied to the nine lognormal distributions to ensure that each variable is weighted equally. Standardization of the data (Xi) results in new values (Zi) that have zero mean and are measured in units of standard deviation (s). The standardized data are obtained by subtracting the mean of the distribution from each data and dividing by the standard deviation of the distribution, Zi = (Xi mean)/s (Davis 1986). Log transformation as well as data standardization is carried out in most of the multivariate statistical analysis (Steinhorst & Williams 1985; Schot & van der Wal 1992; Güler *et al.* 2002).

The cluster analysis in Q mode generated the dendogram of Figure 7(b), where two large groups are observed. They are fundamentally distinguished by the hydrogeochemical features, that is, saline content and geochemical type. Group 1 is characterized by salty waters, with TDS values >3,500 mg/L and sodium chloride, sodium sulphate-chloride and sodium chloride-sulphate geochemical type. Group 2 is characterized by water samples with TDS <3,500 mg/L, corresponding to fresh and brackish water, mostly of the sodium bicarbonate type. This analysis coincides with the two large areas of low $rHCO_3^-/rCl^-$ (Figure 6).

Geomorphology and local aquifer recharge

As has been stated, fixed and remobilized dune bodies (I.1.a. Field of parabolic dunes) are areas of local recharge from rainfalls (Figure 8(a)). This situation and the relationship with water quality was corroborated from the hydrogram

Table 3 | Groundwater physico-chemical analysis (unconfined aquifer, 90 samples)

Sample	pH	EC (μS/cm)	TDS (mg/L)	CO_3 (mg/L)	CO_3H^- (mg/L)	SO_4 (mg/L)	Cl^- (mg/L)	Na^+ (mg/L)	K^+ (mg/L)	Ca^+ (mg/L)	Mg^+ (mg/L)
M2	7.83	1,560	1,092	0.0	725.0	102.5	125.7	391.3	21.5	36.8	27.8
M8	8.00	2,490	1,743	0.0	1,000.0	149.5	185.7	571.3	96.7	32.8	48.3
M9	7.50	700	490	0.0	342.5	31.5	31.4	54.6	13.9	68.0	27.3
M12	8.40	1,900	1,330	48.5	950.0	78.9	51.4	533.9	35.8	11.2	14.1
M14	8.30	3,300	2,310	0.0	1,475.0	196.4	288.6	950.5	23.7	20.0	34.1
M23	8.42	3,800	2,660	14.5	1,485.0	518.0	271.4	1,167.8	27.5	12.8	9.3
M27b	8.08	2,500	1,750	0.0	1,000.0	227.7	142.9	621.8	18.8	28.0	43.9
M35	8.40	2,430	1,701	9.7	835.0	309.5	222.9	697.7	11.9	12.4	11.0
M37	8.98	700	490	24.2	287.5	74.4	17.1	185.0	4.0	6.4	5.9
M39	8.28	1,010	707	0.0	475.0	92.5	40.0	212.3	14.7	32.0	22.9
M43	7.81	3,000	2,100	0.0	815.0	515.2	274.3	611.7	20.8	57.6	116.1
M44	7.34	1,056	739	0.0	415.0	65.3	34.3	68.8	10.8	81.6	59.5
M45	7.98	3,250	2,275	0.0	910.0	302.4	308.6	581.4	18.4	80.0	82.9
M47	8.02	12,100	8,470	0.0	1,500.0	2,053.8	3,142.9	3,791.7	86.2	40.0	79.0
M48	8.11	10,600	7,420	0.0	1,250.0	2,124.7	2,371.4	3,417.6	36.6	64.0	107.3
M49	8.14	8,100	5,670	0.0	750.0	1,915.3	1,720.0	2,517.7	36.3	96.0	121.0
M51	8.23	6,020	4,214	0.0	1,010.0	976.5	1,131.4	1,577.4	25.2	49.6	75.1
M52	8.50	1,300	910	9.7	575.0	63.5	34.3	247.2	8.2	17.6	21.5
M53	8.03	4,400	3,080	0.0	1,125.0	133.8	617.1	835.2	29.3	78.4	62.0
M54	8.26	2,300	1,610	0.0	1,025.0	191.2	68.6	419.6	30.2	14.4	50.7
M55	8.28	3,600	2,520	0.0	755.0	650.2	525.7	906.0	27.5	41.6	53.7
M56	8.26	8,470	5,929	0.0	950.0	1,448.4	2,057.1	2,821.0	37.2	30.4	50.7
M58	8.38	7,000	4,900	2.4	922.5	835.4	1,200.0	2,002.0	33.7	16.0	31.2
M59	8.43	7,990	5,593	24.2	1,325.0	1,287.3	1,600.0	2,578.4	71.5	24.0	45.9
M60a	8.17	12,300	8,610	0.0	800.0	2,495.1	3,485.7	3,842.3	36.0	86.4	163.9
M60b	8.20	14,000	9,800	0.0	1,075.0	2,575.6	3,771.4	4,550.1	38.1	40.0	95.6
M61	8.50	6,000	4,200	9.7	865.0	1,255.1	1,142.9	1,895.9	16.1	19.2	32.2
M62	8.98	2,000	1,400	60.6	987.5	15.7	85.7	551.1	6.4	4.8	13.7
M63	8.8	1,990	1,393	17.0	850.0	158.8	88.6	546.0	9.1	2.4	3.9
M64	7.95	10,800	7,560	0.0	925.0	1,640.0	2,471.4	3,159.8	32.8	41.6	62.4
M65	7.78	8,400	5,880	0.0	675.0	615.4	1,828.6	1,941.4	34.6	46.4	54.6
M67	8.06	3,510	2,457	0.0	840.0	518.0	474.3	844.3	19.9	30.4	46.8
M68	8.52	14,530	10,171	2.4	765.0	1,425.8	3,528.6	3,488.4	97.4	92.8	153.2
M69	8.3	2,020	1,414	0.0	560.0	202.6	177.1	312.4	12.5	49.6	62.4
M70	8.06	1,808	1,266	0.0	590.0	320.2	145.7	424.7	15.4	30.4	49.8
M71a	8.29	4,050	2,835	0.0	575.0	240.5	714.3	728.0	23.4	27.2	42.0
M71b	8.19	6,560	4,592	0.0	622.5	653.0	1,100.0	1,334.7	31.6	43.2	60.5
M72	8.6	3,100	2,170	26.7	880.0	516.6	274.3	763.4	12.2	15.2	12.7
M74	8.3	2,010	1,407	0.0	600.0	339.3	151.4	485.3	8.5	27.2	29.3
M77	8.0	5,350	3,745	0.0	870.0	931.5	1,594.3	1,395.3	38.1	33.6	41.0

(*continued*)

Table 3 | continued

Sample	pH	EC (μS/cm)	TDS (mg/L)	CO_3 (mg/L)	CO_3H^- (mg/L)	SO_4 (mg/L)	Cl^- (mg/L)	$Na+$ (mg/L)	$K+$ (mg/L)	$Ca+$ (mg/L)	$Mg+$ (mg/L)
M79	7.85	1,930	1,351	0.0	660.0	84.4	154.3	312.4	12.0	48.8	58.0
M80a	8.41	1,670	1,169	4.8	737.5	75.3	125.7	400.4	12.0	27.2	22.4
M80b	8.42	3,800	2,660	4.8	1,335.0	267.9	434.3	808.9	36.0	43.2	81.0
M82	7.8	1,700	1,190	0.0	460.0	259.5	222.9	242.7	19.3	80.8	54.6
M83	8.2	1,650	1,155	0.0	800.0	88.0	65.7	385.2	11.4	24.8	26.3
M84	8.64	1,670	1,169	24.2	825.0	92.5	28.6	448.9	8.2	4.8	9.3
M85	8.2	1,950	1,365	0.0	900.0	146.3	85.7	520.7	9.2	7.2	11.2
M86	8.3	1,850	1,295	0.0	715.0	332.7	51.4	348.8	9.1	17.6	14.6
M87	8.6	2,300	1,610	19.4	900.0	333.3	74.3	556.1	8.4	4.0	11.2
M88	8.2	1,900	1,330	0.0	700.0	416.7	80.0	364.0	10.4	29.6	40.5
M89	8.2	2,460	1,722	0.0	685.0	508.2	274.3	632.0	11.0	8.8	15.1
M92	8.5	3,620	2,534	14.5	655.0	705.9	468.6	975.7	13.5	9.6	12.7
M93	7.8	9,370	6,559	0.0	450.0	1,944.3	1,957.1	2,325.6	12.6	112.0	150.7
M94	8.2	4,250	2,975	0.0	1,000.0	499.9	388.6	1,061.7	19.9	21.6	33.7
M95	7.9	8,990	6,293	0.0	545.0	1,543.4	2,057.1	2,042.5	65.6	144.0	165.9
M96	8.2	5,020	3,514	0.0	835.0	714.3	857.1	1,294.2	29.9	44.0	69.3
M97	7.9	9,540	6,678	0.0	700.0	1,867.0	1,828.6	2,548.0	41.8	70.4	77.6
M98	8.6	2,430	1,701	24.2	850.0	264.3	160.0	621.8	14.4	7.2	9.3
M99	7.6	7,600	5,320	0.0	435.0	1,602.9	1,657.1	1,820.0	37.8	222.4	185.4
M101	8.5	1,470	1,029	19.4	705.0	102.5	34.3	321.5	7.0	6.4	13.2
M102	8	14,040	9,828	0.0	835.0	2,565.9	3,171.4	3,731.0	75.0	168.0	204.9
M103a	7.7	650	455	0.0	347.5	32.3	14.3	72.8	19.0	32.0	30.7
M103b	7.7	660	462	0.0	347.5	36.6	14.3	68.8	19.2	31.2	33.7
M105a	8.4	5,740	4,018	12.1	907.5	1,168.2	885.7	1,415.6	28.1	33.6	64.9
M105b	8	6,690	4,683	0.0	1,270.0	1,119.9	1,165.7	1,820.0	33.7	27.2	54.1
M106	8.1	5,230	3,661	0.0	705.0	1,016.8	828.6	1,162.8	32.8	51.2	58.5
M107	7.6	3,580	2,506	0.0	360.0	758.8	562.9	697.7	27.5	100.8	11.2
M108	8	2,480	1,736	0.0	625.0	538.8	154.3	530.8	14.1	24.0	10.2
M109	7.8	7,010	4,907	0.0	1,092.5	1,789.7	942.9	1,718.9	63.9	48.0	85.9
M110	7.5	9,190	6,433	0.0	837.5	1,995.9	1,631.4	2,184.0	74.4	65.6	123.4
M111	8.6	2,580	1,806	14.5	687.5	573.7	162.9	637.0	16.7	17.6	21.5
M113	8	7,740	5,418	0.0	1,507.5	1,606.2	1,028.6	2,047.5	34.9	24.0	34.6
M114	8.6	1,320	924	17.0	487.5	160.9	40.0	311.4	6.6	12.0	10.2
M115	8.3	720	504	0.0	425.0	29.9	17.1	163.8	5.1	13.6	8.8
M116a	8	1,108	776	0.0	395.0	154.7	114.3	242.7	16.3	29.6	30.7
M116b	7.91	3,530	2,471	0.0	415.0	754.7	514.3	728.0	14.2	48.0	57.6
M117a	8.5	1,760	1,232	12.1	752.5	217.2	71.4	482.3	8.5	9.6	13.7
M117b	8.8	4,620	3,234	72.7	1,695.0	217.2	177.1	879.7	123.1	32.0	39.0
M118	8.6	2,970	2,079	38.8	935.0	206.8	205.7	551.1	39.6	34.4	37.6
M120	8.17	5,470	3,829	0.0	925.0	1,287.3	857.1	1,425.7	20.1	15.2	34.6

(*continued*)

Table 3 | continued

Sample	pH	EC (μS/cm)	TDS (mg/L)	CO_3 (mg/L)	CO_3H^- (mg/L)	SO_4 (mg/L)	Cl^- (mg/L)	Na^+ (mg/L)	K^+ (mg/L)	Ca^+ (mg/L)	Mg^+ (mg/L)
M121	8.01	1,600	1,120	0.0	745.0	102.5	57.1	354.9	10.3	21.6	15.1
M122	8	4,700	3,290	0.0	850.0	1,110.2	600.0	1,107.2	48.6	52.0	51.2
M123	7.93	9,130	6,391	0.0	1,375.0	1,738.2	1,285.7	2,406.5	28.7	32.8	33.7
M128	8.5	5,450	3,815	24.2	1,275.0	754.7	857.1	1,314.5	49.2	14.4	28.3
M129	8.55	3,730	2,611	24.2	1,125.0	250.0	342.9	940.3	22.3	9.6	23.4
M130	8.6	2,100	1,470	14.5	557.5	511.0	137.1	566.2	17.4	12.0	15.1
M131	8.24	1,198	839	0.0	620.0	102.5	62.9	273.0	8.8	14.4	13.2
M132	8.24	1,270	889	0.0	575.0	102.5	57.1	291.2	12.9	18.4	11.2
M133	8.77	1,410	987	26.7	542.5	102.5	85.7	291.2	10.8	21.6	15.1
M134	7.47	6,820	4,774	0.0	1,012.5	997.5	1,200.0	1,698.7	49.8	56.8	32.7

Table 4 | Descriptive statistical parameters for 90 groundwater samples (unconfined aquifer)

Parameters	N	Range	Minimum	Maximum	Medium	Deviation tip.
ph	90	1.64	7.34	8.98	8.19	0.34
EC	90	13,880.00	650.00	14,530.00	4,418.55	3,439.62
TDS	90	9,716.00	455.00	10,171.00	3,093.00	2,407.72
CO_3^{-2}	90	72.70	0.00	72.70	6.86	13.54
HCO_3^-	90	1,407.50	287.50	1,695.00	819.88	299.87
SO_4^{-2}	90	2,559.90	15.70	2,575.60	689.99	688.72
Cl^-	90	3,757.10	14.30	3,771.40	727.80	913.83
Na^+	90	4,495.50	54.60	4,550.10	1,135.23	1,020.88
K^+	90	119.10	4.00	123.10	27.70	22.60
Ca^{+2}	90	220.00	2.40	222.40	39.41	36.17
Mg^{+2}	90	201.00	3.90	204.90	48.80	42.89

of the water level obtained in the monitored well (M116) located in the dune beside the Laguna Oscura lagoon. In the water table hydrogram, typical increasing peaks during summer can be observed after the occurrence of the rainfalls. In the same periods the greatest aquifer recharge occurred. Using the water table fluctuation method, the annual recharge to the aquifer was estimated in the order of 10% of the total annual precipitation (Bécher Quinodóz *et al.* 2016). In Figure 9 the annual precipitation and aquifer recharge trend is shown for the dune area (Bécher Quinodóz *et al.* 2016). This aspect influences the chemical composition of groundwater since recharge leads to the development of freshwater lenses in the upper part of the aquifer, given the difference in density with salt water. In this sector, the increase in salinity with depth could be verified. Thus, in the first 5–10 m of the aquifer, the salinity was less than 1 g/L, while at 44 meters the salinity was 2.5 g/L (Figure 8(b)). Previous regional research (Bécher Quinodóz *et al.* 2016), supported by numerical models, indicates the existence of different flow hierarchies explaining situations of water mixing that results in diverse water salinities in the geomorphological units. This is an important finding because a knowledge of the different herarchies of flow systems and the final quality of water mixtures is a basis for designing future wells and for better aquifer use and management.

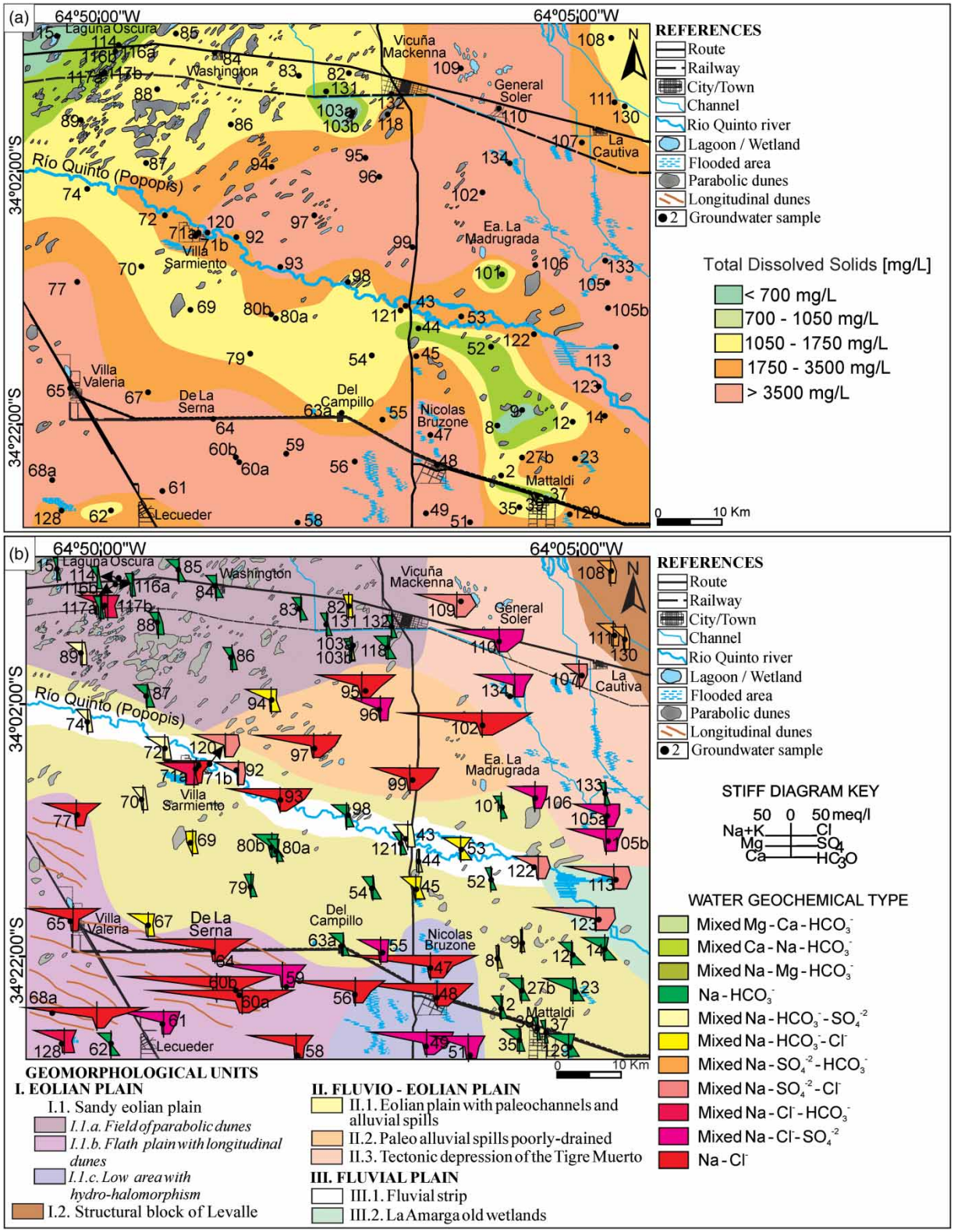

Figure 5 | (a) Spatial distribution of groundwater salinity in the unconfined aquifer; (b) map with Stiff diagrams showing spatial changes in the geochemical type.

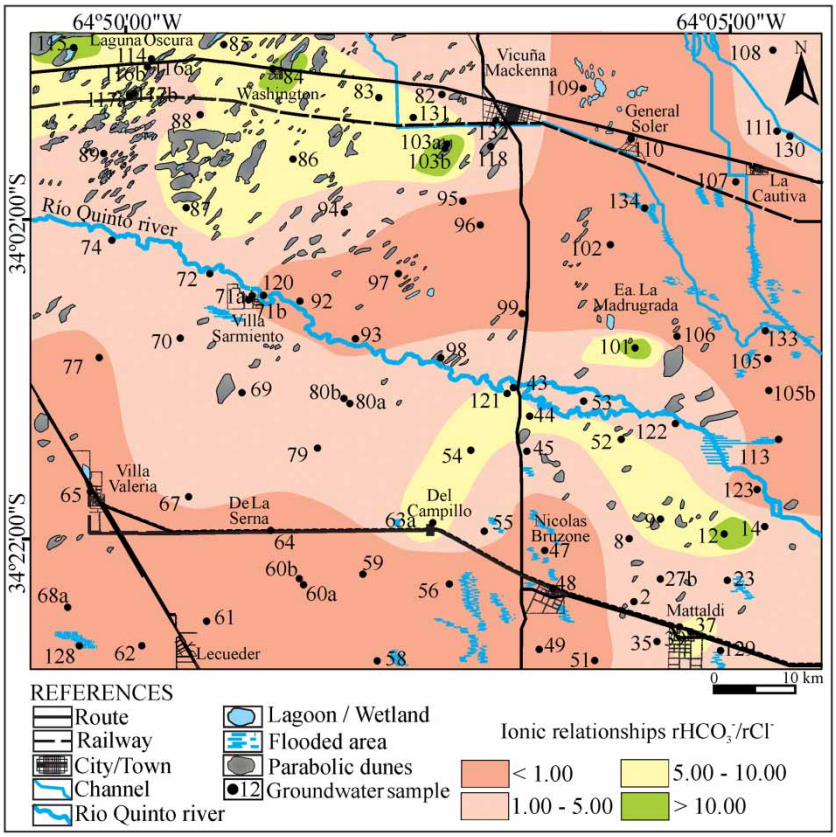

Figure 6 | Map of the relationships $rHCO_3^-/rCl^-$.

CONCLUSIONS

A multifaceted study of the sandy plain of southern Córdoba (Argentina) has been carried out with the objective of characterizing the unconfined aquifer. The study encompassed climate, geomorphology, hydrogeology, hydrodynamics and hydrogeochemistry of the area.

The area presents a landscape with a macro-structural control and an alternating history of wet and dry cycles. The driest ones are characterized by deflation and fundamentally by eolian aggradation with dune formation. The wettest cycles showed fluvial activity, installation of lagoons and wetland and pedogenesis in the interfluvial areas. The result is a composite landscape where different types of dunes coexist with the fluvial environment of the Rio Quinto River.

The hydrogeological study made it possible to define an unconfined aquifer with a thickness of approximately 80 m, consisting mainly of eolian Quaternary sediments (very fine silty sands) with different carbonate cementation degrees. In a subordinated way, fluvial sediments of generally medium to fine textures with disseminated gravels are recognized which are related to paleochannels of the Rio Quinto River. The base of this aquifer is constituted by aquitard materials (very fine sands cemented with carbonates or silty and clayed sands). The results show that the water table depth and its topography, the flow direction, the hydraulic gradients and groundwater velocities are fundamentally conditioned by the relief and by lithological changes. Taking into account the regional setting, the studied area behaves as a transit zone of the groundwater flow coming from the western mountainous and piedmont region. The convergence of intermediate and regional flows in the topographic low sectors generates hydrological discharge areas.

The hydrogeochemical study showed that groundwater, with salinity between 0.4 g/L (fresh) to 10 g/L (salty),

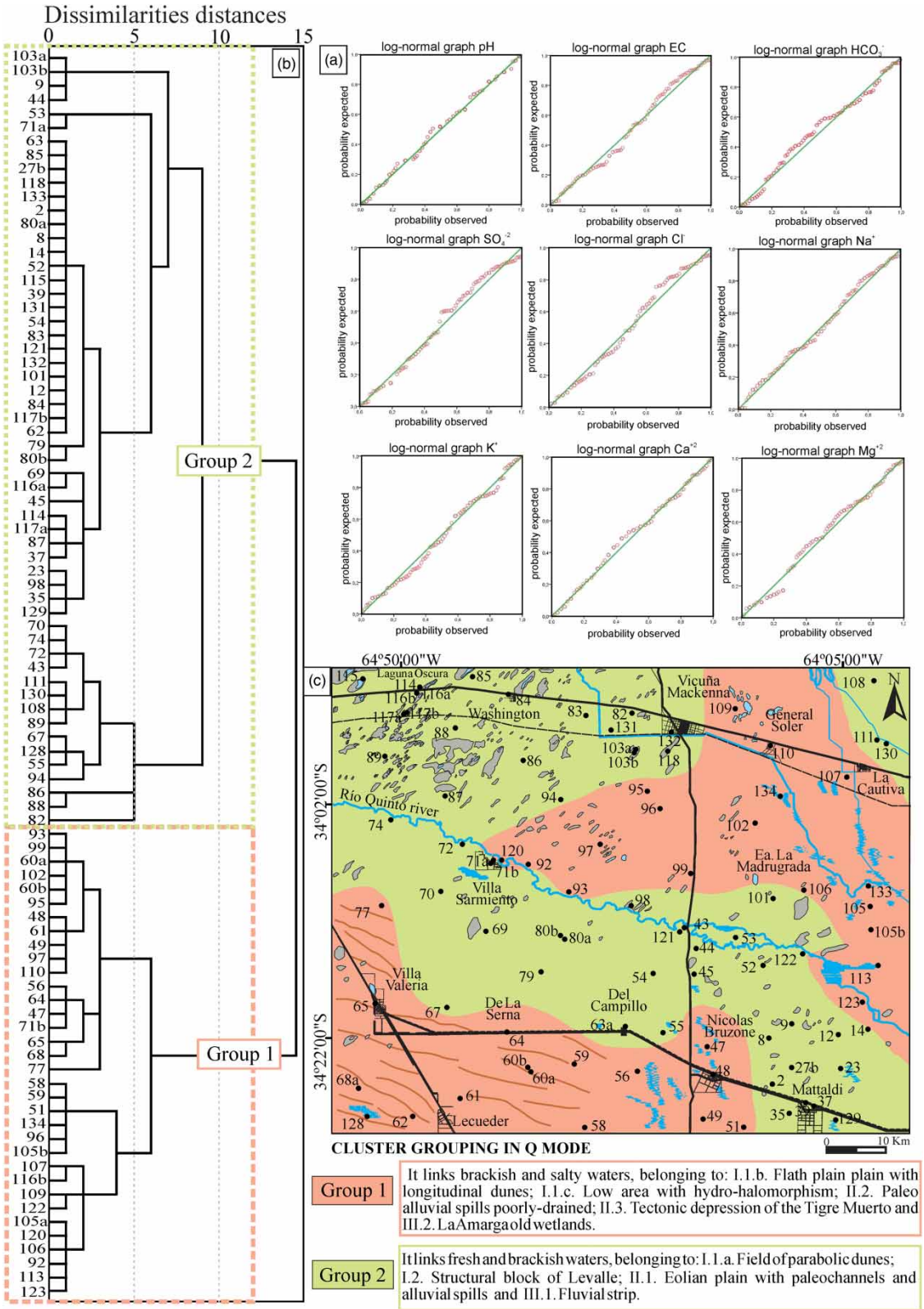

Figure 7 | (a) Statistical distribution of the parameters; (b) clustering in Q mode; (c) map of the cluster grouping in Q mode.

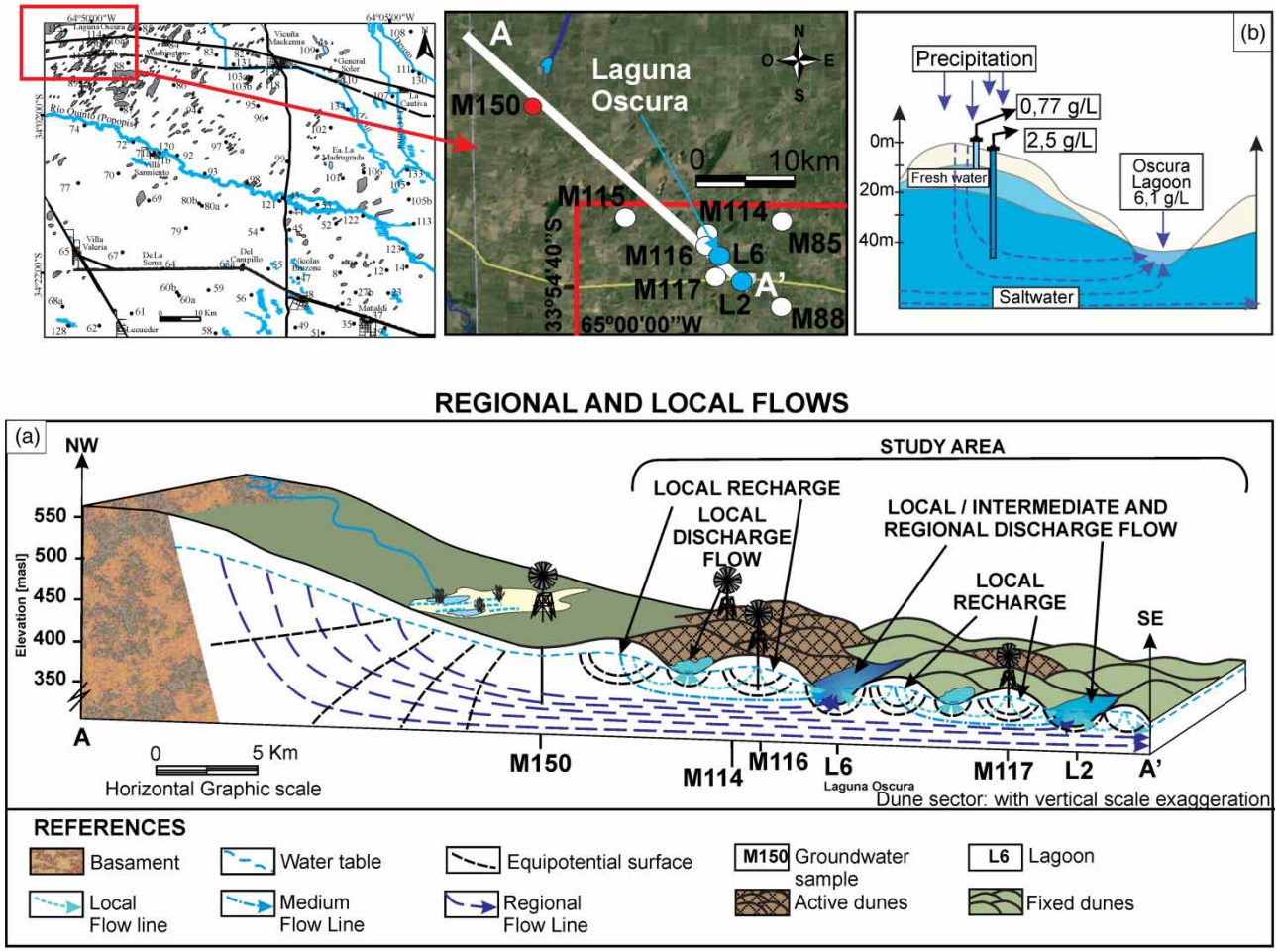

Figure 8 | (a) Regional and local groundwater flow systems in the study area; (b) variation of groundwater salinity with depth in the Laguna Oscura sector.

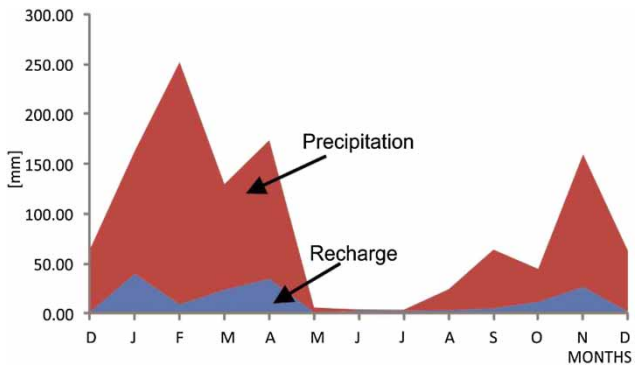

Figure 9 | Evolution of groundwater recharge and precipitation for 12 months. (12/2014–12/2015) after Bécher Quinodóz et al. (2016).

constitutes a varied spatial geochemical pattern. Groundwater is of the calcium bicarbonate, sodium sulfate and sodium chloride types, many of them of mixed anionic type. The salinity and the geochemical type pattern are controlled by the relief and the lithology and the spatial distribution is varied depending on the specific influence of the two factors on each geomorphological unit. To probe the controlling factors all the chemical variables were analyzed together using a statistical multivariate analysis in Q mode, which is useful to explain the spatial variability of chemical species and their relationships. Thus, from the two large groups found in the cluster analysis, the close relationship between the groundwater quality and geomorphological environments may be corroborated. In Group 1, brackish and salty water, of sodium sulfate and chloride type, are considered to be the result of a long transit of intermediate and regional flows, coming from the western sector. In addition, they may be locally controlled by the flatter or depressed relief, by the domain of

fine sediments and by low hydraulic gradients and low groundwater velocity. This situation leads to a long contact time between water and sediment and, consequently, the increase of ions and compounds in solution. In Group 2, bicarbonate fresh waters were linked to local reliefs like active dunes and topographic hills where local flow systems are developed as a result of preferential recharge from precipitation. Also bicarbonate fresh waters appear in areas with coarse sediments of fluvial origin where the higher flow velocity diminishes the ions transference to the solution.

The results obtained allow us to identify the most promising areas to carry out future local studies, contributing to a deeper assessment of groundwater aptitude and the quantification of freshwater resources available for use.

ACKNOWLEDGEMENTS

The research was supported by FONCYT and MINCYT (PID 35/08 Prestamo BID). The National Scientific and Technical Research Council (CONICET) is appreciated.

REFERENCES

Álvarez, M. P., Hernandez, M. A. & Ariztegui, D. 2014 Geomorphological and sedimentological influences in groundwater hydrodynamics: An example from Península Valdés, Patagonia, Argentina. In: *Twenty-second Meeting of Swiss Sedimentologist – Frioburg*, February 22, 2014. Abstracts 6–7. Available from: www.unifr.ch/geoscience/geology/assets/files/SwissSed/Abstractbook_2014.pdf#page=19.

Bécher Quinodóz, F. N. 2014 *Environmental Implications of Hydrodynamic and Hydrochemical Relationships Between Surface Water and Groundwater in the Sandy Plain South of Córdoba, Argentina*. PhD thesis, National University of Río Cuarto (unpublished), Río Cuarto, Córdoba, p. 412.

Bécher Quinodóz, F., Blarasin, M., Cabrera, A., Eric, C. & Felizzia, J. 2016 Groundwater dynamics and recharge assessment in an unconfined aeolian sand aquifer. *Int. J. New Technol. Res. (IJNTR)* **2** (5), 144–149.

Blarasin, M., Cabrera, A., Bécher Quinodóz, F., Felizzia, J. & Giuliano Albo, M. J. 2013 The incidence of relief studies in the finding of water for human supply in the Dune Plain of Cordoba. In: *Groundwater Strategic Resource*, Vol. I (N. González, E. Kruse, M. M. Trovatto & P. Laurencena, eds). EDULP, La Plata, pp. 218–225.

Blarasin, M., Cabrera, A. & Matteoda, E. 2014 *Groundwater in Cordoba Province*, 1st edn. Universidad Nacional Río Cuarto (UNIRIO), Cordoba, Argentina.

Cantú, M. 1992 Holocene in Córdoba Province, in Manual: Holocene in the Argentine Republic. International Symposium on the Holocene in South America, Paraná 1992, T (I) 24.

Carignano, C., Kröhling, D., Degiovanni, S. & Cioccale, M. 2014 Geomorphology of Cordoba Province (Argentina). In: *XIX Argentine Geological Congress* (R. Martino & A. Guereschi, eds). Geological Association of Argentina, Argentina, pp. 747–822.

Carol, E., Kruse, E. & Roig, A. 2010 Groundwater travel time in the freshwater lenses of Samborombón Bay, Argentina. *Hydrol. Sci. J.* **55** (5), 754–762.

Carol, E., García, L. & Borzi, G. 2015 Hydrogeochemistry and sustainability of freshwater lenses in the Samborombón Bay wetland, Argentina. *J. South Am. Earth Sci.* **60**, 21–30.

Chakraborty, S., Dutta, T. & Sikdar, P. K. 2011 Understanding the control of geology, geomorphology and landuse/landcover on arsenic distribution in groundwater of Bengal Basin using RS, GIS and PCA. *Survey* **52** (3&4), 70–85.

Cloutier, V., Lefebvre, R., Therrien, R. & Savard, M. M. 2008 Multivariate statistical analysis of geochemical data as indicative of the hydrogeochemical evolution of groundwater in a sedimentary rock aquifer system. *J. Hydrol.* **353** (3–4), 294–313.

Criado, R. P., Mombrú, C. & Ramos, V. 1981 Structure and tectonic interpretation. In: *VIII Argentine Geological Congress*. San Luis, pp. 155–192.

Custodio, E. 1993 Hydrogeochemistry and environmental Isotopes. In: *Current Topics of Underground Hydrology* (E. Bocanegra & A. Rapaccini, eds). National University of Mar del Plata and Federal Investment Council, Mar del Plata, pp. 61–78.

Davis, J. C. 1986 *Statistics and Data Analysis in Geology*. John Wiley & Sons Inc., New York.

Degiovanni, S., Villegas, M., Blarasin, M. & Sagripanti, G. 2005 *Geological Map 3363-III*. National Mining Secretariat, Río Cuarto.

Del Pilar Álvarez, M., Weiler, N. E. & Hernández, M. A. 2010 Linking geomorphology and hydrodynamics: a case study from Peninsula Valdés, Patagonia, Argentina. *Hydrogeol. J.* **18** (2), 473–486.

Güler, C., Thyne, G. D., McCray, J. E. & Turner, A. K. 2002 Evaluation of graphical and multivariate statistical methods for classification of water chemistry data. *Hydrogeol. J.* **10**, 455–474.

Iriondo, M. 1990 Climatic changes in the South American plains: records of a continent-scale oscillation. *Quat. Int.* **57**, 93–112.

Kostadinoff, J. & Gregori, D. A. 2004 Mercedes geological basin, San Luis province. *J. Geol. Assoc. Argentina* **59** (3), 488–494.

Rajaveni, S. P., Brindha, K. & Elango, L. 2017 Geological and geomorphological controls on groundwater occurrence in a hard rock region. *Appl. Water Sci.* **7** (3), 1377–1389.

Ramaiah, S. N., Gopalakrishna, G. S., Vittala, S. S. & Najeeb, K. M. 2012 Geomorphological mapping for identification of ground water potential zones in hard rock areas using geo-spatial information – a case study in Malur Taluk, Kolar District, Karnataka, India. *Nature Environ. Pollut. Technol.* **11** (3), 369–376.

Rani, V. R., Pandalai, H. S., Sajinkumar, K. S. & Pradeepkumar, A. P. 2015 Geomorphology and its implication in urban groundwater environment: case study from Mumbai, India. *Appl. Water Sci.* **5** (2), 137–151.

Schot, P. P. & van der Wal, J. 1992 Human impact on regional groundwater composition through intervention in natural flow patterns and changes in land use. *J. Hydrol.* **134**, 297–313.

Sedhuraman, M., Revathy, S. S. & Babu, S. S. 2014 Integration of geology and geomorphology for groundwater assessment using remote sensing and GIS techniques. *Int. J. Innov. Res. Sci. Eng. Technol.* **3** (3), 71–85.

Steinhorst, R. K. & Williams, R. E. 1985 Discrimination of groundwater sources using cluster analysis, MANOVA, canonical analysis and discriminant analysis. *Water Resour. Res.* **21**, 1149–1156.

Tóth, J. 1999 Groundwater as a geologic agent: an overview of the causes, processes, and manifestations. *Hydrogeol. J.* **7** (1), 1–14.

Tripaldi, A. & Forman, S. L. 2007 Geomorphology and chronology of Late Quaternary dune fields of western Argentina. *Palaeogeogr. Palaeoclimatol. Palaeoecol.* **251** (2), 300–320.

First received 17 March 2018; accepted in revised form 14 September 2018. Available online 9 October 2018